

STAR FORMATION IN M33 (HERM33ES)

C. Kramer¹, M. Boquien², J. Braine³, C. Buchbender¹, D. Calzetti²,
P. Gratier⁴, B. Mookerjee⁵, M. Relaño⁶ and S. Verley⁶

Abstract. Within the key project “Herschel M33 extended survey” (**HerM33es**), we are studying the physical and chemical processes driving star formation and galactic evolution in the nearby galaxy M33, combining the study of local conditions affecting individual star formation with properties only becoming apparent on global scales. Here, we present recent results obtained by the **HerM33es** team. Combining Spitzer and Herschel data ranging from $3.6\,\mu\text{m}$ to $500\,\mu\text{m}$, along with H I, H α , and GALEX UV data, we have studied the dust at high spatial resolutions of 150 pc, providing estimators of the total infrared (TIR) brightness and of the star formation rate. While the temperature of the warm dust at high brightness is driven by young massive stars, evolved stellar populations appear to drive the temperature of the cold dust. Plane-parallel models of photon dominated regions (PDRs) fail to reproduce fully the [C II], [O I], and CO maps obtained in a first spectroscopic study of one $2' \times 2'$ subregion of M33, located on the inner, northern spiral arm and encompassing the H II region BCLMP 302.

1 Introduction

M33 is a nearby galaxy located at only 840 kpc with a moderate inclination of 56° , actively forming stars. It has been studied at radio, optical and X-ray wavelengths. Its metallicity is about half solar, similar to the LMC. Using Herschel, M33 provides an exceptional physical resolution of ~ 50 pc at $158\,\mu\text{m}$ allowing us to resolve the various morphological components of the galaxy. The absence of an active nucleus excludes one possible dust heating mechanism and the shallow

¹ IRAM, Av. Divina Pastora 7, Nucleo Central, E-18012 Granada, Spain

² Department of Astronomy, University of Massachusetts, Amherst, MA 01003, USA

³ Observatoire de Bordeaux, OASU, UMR 5804, CNRS/INSU, Floirac F-33270

⁴ IRAM, 300 rue de la Piscine, 38406 St. Martin d'Hères, France

⁵ Tata Institute of Fundamental Research, Homi Bhabha Road, Mumbai 400005, India

⁶ Dept. Física Teórica y del Cosmos, Universidad de Granada, Granada, Spain

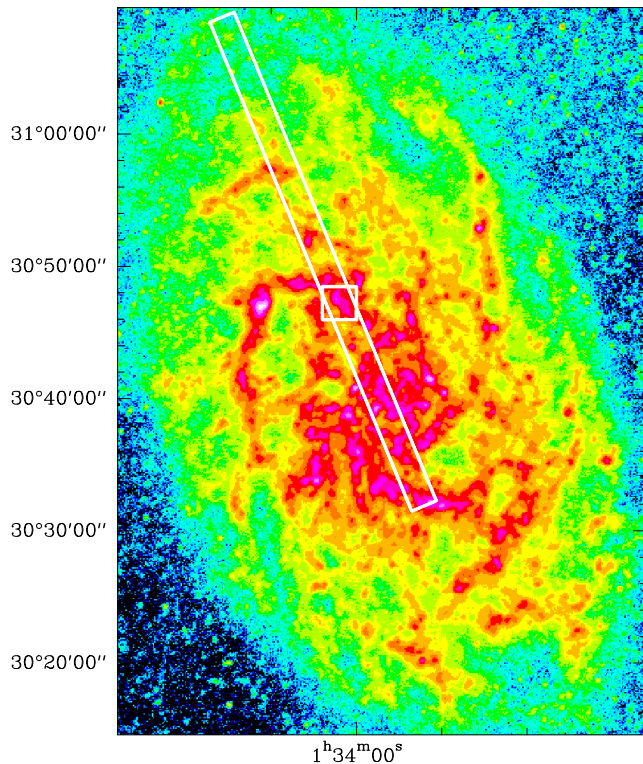


Fig. 1. SPIRE 250 μm map of M33 (Kramer et al. 2010). The tilted rectangle delineates the $2' \times 40'$ wide strip along the major axis, which will be partially mapped with HIFI and PACS in spectroscopy mode. The $2' \times 2'$ box delineates the region mapped in [C II] and [O I] by Mookerjea et al. (2011) and shown in Figure 3.

metallicity gradient limits the influence of the radial evolution of the metallicity on the emission of the dust. In a first step to study the interstellar medium and its interplay with star formation, we mapped the dust spectral energy distribution over the entire galaxy using SPIRE and PACS (Kramer et al. 2010, Verley et al. 2010, Braine et al. 2010, Boquien et al. 2010, 2011).

In a second step, we have started to use PACS and HIFI to map the emission of [C II] and other strong far-infrared (FIR) lines along the major axis of M33 (Mookerjea et al. 2011). Observing an extended strip, will allow us to study the ionized, atomic, and molecular phases of the interstellar medium, its life cycle and thermal balance, tracing the formation of molecular clouds and of stars.

Here, we summarize the major results obtained in two recently submitted papers of the **HerM33es** team. But note that only 8 hours out of the total granted 191 hours of Herschel observing time were observed till end of 2010.

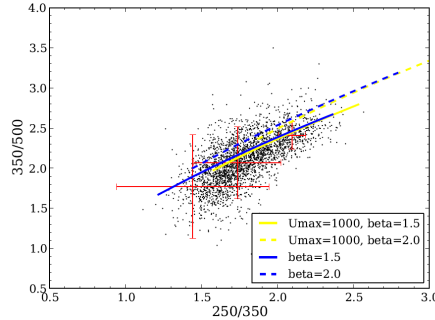


Fig. 2. The observations of the SPIRE bands can be reproduced by the Draine & Li (2007) models (Boquien et al. 2011). Here, we consider a single illuminating radiation field or a radiation field ranging from an arbitrary U_{\min} to $U_{\max}=1000$, with U the radiation field in the solar neighborhood. Even if the scatter is large, an emissivity index of $\beta = 1.5$ fits the observations very well, in accordance with the results obtained from the radial averages studied by Kramer et al. (2010).

2 Dust heating sources in galaxies: the case of M33

Dust emission in galaxies can have several unrelated origins: (1) Massive stars in star-forming regions heat the dust. (2) A large scale diffuse emission due to cirrus being heated by (a) energetic radiation escaping from individual star-forming regions and/or (b) the general radiation field of evolved stars. (3) Hot grains in the photosphere or circumstellar atmosphere of mass-losing stars also contribute.

IR emission acts as a star-formation tracer even at high redshifts. As the diffuse emission can represent up to nearly 90% of the IR flux in Sa galaxies, it can lead to an error on the SFR up to an order of magnitude depending on its origin.

In Boquien et al. (2011), we have used Herschel PACS and SPIRE observations in combination with Spitzer IRAC and MIPS data, GALEX FUV data, as well as ground-based $H\alpha$ and HI maps of M33, in order to characterize the warm and cold dust populations. Given the high spatial resolution of even the longest wavelength bands (~ 150 pc at $500\mu\text{m}$), we perform a pixel-to-pixel analysis of the data in order to constrain the dust heating sources. To do so, we have convolved all the data to the resolution of the SPIRE $500\mu\text{m}$ band. The maps have then been registered to common pixels of a size of $42''$. For the analysis, only pixels with a signal-to-noise ratio of at least 3 have been selected. The limiting factor is here the PACS bands which are relatively shallow. In the subsequent analysis at least ~ 850 pixels have been selected in each case.

We have studied the evolution of the dust colors both as a function of the position in the galaxy (including the radial distance) and the brightness.

To determine the TIR luminosities, we have fitted the models of Draine & Li (2007) to the SED of each spatial pixel from $8\mu\text{m}$ to $500\mu\text{m}$ and integrated the model from $1\mu\text{m}$ to 1mm . In addition, we derived the star formation rate

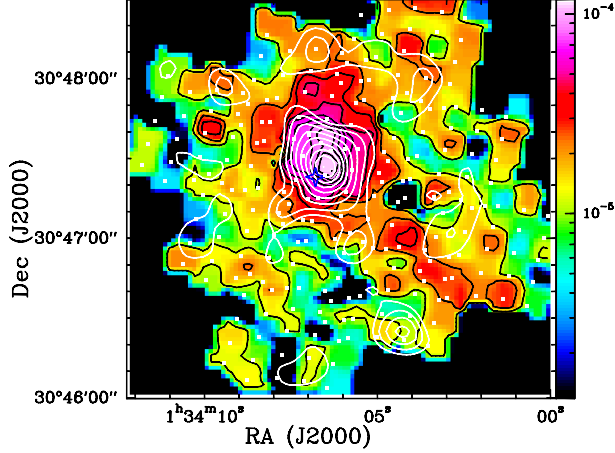


Fig. 3. Maps of $158\,\mu\text{m}$ [C II] (in color and black contours) and $63\,\mu\text{m}$ [O I] (white contours) emission observed with PACS toward the H II region BCLMP 302 in M33 (shown as small box in Figure 1). The $\text{H}\alpha$ peak observed with HIFI is marked with the asterisk (cf. Fig. 4). The white dots show the footprint of the PACS observations. Both images are at a common resolution of $12''$.

(SFR) from Calzetti et al. (2007) combining $\text{H}\alpha$ and the $24\,\mu\text{m}$ emission. Plotting the derived SFR against just one IR band, we find that the emission at $8\,\mu\text{m}$ is sublinear, confirming previous results. The emission near the peak of the emission between $70\,\mu\text{m}$ and $160\,\mu\text{m}$ is a linear estimator of the SFR. Finally, the emission in SPIRE bands is an increasingly super linear estimator of the SFR with an ever larger scatter around the best fit.

In summary, we found the following results:

1. The colors of the warm and cold dust components seem to be predominantly driven by the evolution of the radiation field.
2. Combining any set of Spitzer and Herschel bands, we have provided correlations to estimate both the TIR brightness and the SFR, extending the results of Boquien et al. (2010) and Verley et al. (2010), which is of importance for the study of high redshift galaxies.
3. The color trends of the warm and the cold dust show that they are heated by different sources. At higher SFR, the warm dust temperature seems to be driven by star formation. As star formation weakens, the temperature is increasingly driven by another component, most likely the evolved stellar populations. The cold dust temperature seems to be driven by the old stellar population, with a tight correlation with the local stellar mass.

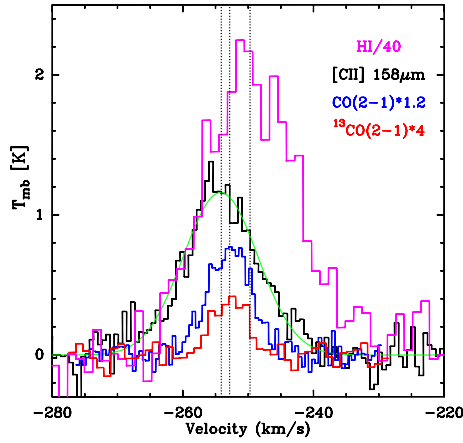


Fig. 4. Spectra of [C II], H I, CO and ^{13}CO 2–1 at the $\text{H}\alpha$ peak position of the H II region BCLMP 302. All four spectra are at $\sim 12''$ resolution.

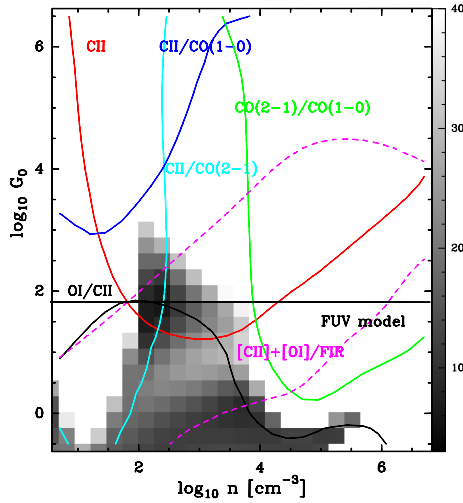


Fig. 5. Comparison of line intensities and intensity ratios at the position of the $\text{H}\alpha$ peak with plane-parallel constant density PDR models (Kaufman et al. 1999) of different density n and FUV field, G_0 . Grey-scalés show the estimated reduced χ^2 . The horizontal line shows the FUV estimated from the TIR intensity.

3 [C II] and [O I] at 50 pc scales in the northern arm of M33

In Mookerjee et al. (2011), we have used PACS on Herschel to observe the emission of the far-infrared lines [C II] ($158\,\mu\text{m}$), [O I] ($63\,\mu\text{m}$), [N II] ($122\,\mu\text{m}$), [N III] ($57\,\mu\text{m}$) in a $2' \times 2'$ region of the northern spiral arm of M33, centered on the H II region

BCLMP 302 (Figure 3).

At the peak of $H\alpha$ emission, we have observed in addition a velocity resolved $[C\ II]$ spectrum using HIFI (Figure 4). The aim of this work is to understand the relative contributions of the different phases of the ISM to $[C\ II]$ cooling, as well as the correlation of the $[C\ II]$ emission with the star formation rate (SFR), derived from $H\alpha$ and $24\ \mu\text{m}$ emission observed with Spitzer, at scales of $12''$ corresponding to $\sim 50\text{ pc}$, i.e. at scales of individual giant molecular clouds (GMCs). We have obtained the distribution of $[C\ II]$ and $[O\ I]$ ($63\ \mu\text{m}$) emission from the spiral arm and the inter-arm regions, and detected the $[N\ II]$ ($122\ \mu\text{m}$) and $[N\ III]$ ($57\ \mu\text{m}$) lines at several positions. These data are quantitatively compared with continuum maps observed with PACS $100\ \&\ 160\ \mu\text{m}$ and of CO and H I data, at the same resolution.

The $[C\ II]$ emission shows strong correlation with the TIR intensity only within the H II region and is well correlated with SFR along the spiral arm. The gas heating efficiency, estimated as the ratio between $[C\ II]$ and the TIR continuum, varies between 0.07 and 2%. We used the CLOUDY models of ionized and photon dominated regions (Ferland et al. 1998) and the known properties of BCLMP 302, to estimate that upto 30% of the $[C\ II]$ emission stems from the H II region. Next, we used plane-parallel constant density PDR models of Kaufman et al. (1999), to interpret the observed intensities of far-infrared and millimeter lines at the $H\alpha$ position (Figure 5). Both, the FIR continuum and results of PDR modeling indicate that a FUV field of $\sim 50\ G_0$ is heating the dust and gas at the $H\alpha$ peak position. Over the surface of the studied region, the bulk of $[C\ II]$ emission originates from PDRs at cloud surfaces, while the contributions from the atomic and molecular medium account for less than 10% of the observed $[C\ II]$ emission.

The rather poor fit of the intensity ratios towards the $H\alpha$ peak shows the shortcomings of a plane-parallel single density PDR model. First tests using KOSMA- τ PDR models (Röllig et al. 2006) of spherical clumps with density gradients do better reconcile the observations. In a forthcoming paper, we shall discuss new HIFI $[C\ II]$ data at other positions in the BCLMP 302 region using much more detailed PDR models, also taking into account the effects of sub-solar metallicity.

References

- Boquien, M., Calzetti, D., Kramer, C. *et al.* 2010, A&A, 518, 70
- Boquien, M., Calzetti, D., Combes, F. *et al.* 2011, AJ, submitted
- Braine, J., Gratier, P., Kramer, C. *et al.* 2010, A&A, 518, 69
- Calzetti, D., Kennicutt, R.C., Engelbracht, C.W. *et al.* 2007, ApJ, 666, 870
- Draine, B.T., Li, A. 2007, ApJ, 657, 810
- Ferland, G. J., Korista, K. T., Verner, D. A., *et al.* 1998, PASP, 110, 761
- Kaufman, M. J., Wolfire, M. G., Hollenbach, D. J., *et al.* 1999, ApJ, 527, 795
- Kramer, C., Buchbender, C., Xilouris, E.M. *et al.* 2010, A&A, 518, 67
- Mookerjee, B., Kramer, C., Buchbender, C. *et al.* 2011, A&A, submitted
- Röllig, M., Ossenkopf, V., Jeyakumar, S. *et al.* 2006, A&A, 451, 917
- Verley, S., Relaño, M., Kramer, C. *et al.* 2010, A&A, 518, 68